Soil CO₂ venting as one of the mechanisms for tolerance of Zn deficiency by rice in flooded soils

MARIE-CECILE AFFHOLDER[1], DOMINIK J. WEISS[2], MATTHIAS WISSUWA[3], SARAH E. JOHNSON-BEEBOUT[4] & GUY J.D. KIRK[1]

[1]School of Water, Energy and Environment, Cranfield University, Cranfield MK43 0AL, UK;

[2]Department of Earth Science and Engineering, Imperial College London, London SW7 2AZ, UK;

[3]Crop Production and Environment Division, Japan International Research Center for Agricultural Sciences, 1-1 Ohwashi, Tsukuba, Ibaraki 305-8686, Japan; [4]Crop and Environmental Sciences Division, International Rice Research Institute, DAPO BOX 7777, Metro Manila, Philippines

Correspondence: Guy Kirk, e-mail g.kirk@cranfield.ac.uk

ABSTRACT

We sought to explain rice (*Oryza sativa*) genotype differences in tolerance of zinc (Zn) deficiency in flooded paddy soils and the counter-intuitive observation, made in earlier field experiments, that Zn uptake per plant increases with increasing planting density. We grew tolerant and intolerant genotypes in a Zn-deficient flooded soil at high and low planting densities, and found (a) plant Zn concentrations and growth increased with planting density and more so in the tolerant genotype, whereas the concentrations of other nutrients decreased, indicating a specific effect on Zn uptake; (b) the effects of planting density and genotype on Zn uptake could only be explained if the plants induced changes in the soil to make Zn more soluble; and (c) the genotype and planting density effects were both associated with decreases in dissolved CO_2 in the rhizosphere soil solution and resulting increases in pH. We suggest the increases in pH caused solubilisation of soil Zn by dissolution of alkali-soluble, Zn-complexing organic ligands from soil organic matter. We conclude that differences in venting of soil CO_2 through root aerenchyma were responsible for the genotype and planting density effects.

Key-words: dissolved CO_2, genotype nutrient uptake differences, rhizosphere pH, zinc solubilisation

We provide evidence for a previously unexplored mechanism to explain rice genotype differences in tolerance of Zn deficiency: venting of soil CO2 through root aerenchyma, resulting in solubilisation of soil Zn and hence increased plant uptake. Large concentrations of dissolved CO2 develop in flooded paddy soils as respiratory CO2 accumulates, and this can cause extreme insolubility of Zn and hence Zn deficiency in rice crops and grain. We show that venting of CO2 via root aerenchyma leads to changes in soil chemistry that make Zn more soluble, and that this can account for genotype differences in Zn uptake and also the counter-intuitive finding that uptake increases with increasing plant density. We do this with measurements of uptake and simultaneous changes in rhizosphere chemistry, analysed with a mathematical model.

INTRODUCTION

Deficiency of zinc (Zn) is one of the main soil constraints to rice production (Dobermann & Fairhurst 2000) and Zn is often deficient in human populations with rice-based diets (IRRI 2010). These are particular problems in rice because the anoxic conditions that develop in flooded paddy soils mean Zn solubility and hence plant uptake are impaired. Tolerance of the deficiency and ability to concentrate Zn in grains are priorities in current rice breeding programmes (Slamet-Loeden *et al.* 2015). There are large differences in the rice germplasm in tolerance of the deficiency (Quijano *et al.* 2002; Wissuwa *et al.* 2006), related to differences in root growth irrespective of Zn uptake, and in uptake per unit root growth (Rose *et al.* 2013; Mori *et al.* 2016). However the specific mechanisms involved are poorly understood and this impedes progress in breeding.

The differences in uptake per unit root growth are linked to root-induced changes in the soil (Mori *et al.* 2016). Evidence for this includes the counter-intuitive finding that uptake per plant increases when plants are grown closer together (Hoffland *et al.* 2006; Mori *et al.* 2016). More closely-spaced plants will compete with each other for Zn in the soil. However they may also benefit each other if there is a synergistic interaction between neighbouring roots, resulting in increased solubility of soil Zn or neutralization of a toxin or both. Earlier work (Arnold *et al.* 2010; Ptashnyk *et al.* 2011; Marković *et al.* 2017) led us to propose secretion of Zn solubilising phytosiderophores from the roots and uptake of Zn-phytosiderophore complexes to explain rice genotype differences and the planting density effect. However we have so far failed to consistently detect enhanced phytosiderophore secretion from tolerant genotypes.

An alternative mechanism, which so far has not received attention, is the venting of soil CO_2 through the roots (Fig. 1, Process 2). Large concentrations of dissolved CO_2 (equivalent partial pressures 5–70 kPa –Ponnamperuma 1972; Greenway *et al.* 2006) develop in submerged rice soils because CO_2 formed in microbial respiration escapes only slowly by diffusion through the water-saturated soil pores, diffusion in water being 10^4 times slower than diffusion in air. CO_2 is produced in anaerobic respiration in the soil bulk and in aerobic respiration in the rhizosphere fuelled by O_2 and organic substrates released from the roots (Fig. 1, Process 1). There is therefore a large CO_2 gradient

between the soil and the gas channels (aerenchyma) inside the root, by which the root is aerated. Hence CO_2 may be taken up by the roots and vented to the atmosphere by diffusion through the root aerenchyma (Higuchi 1982; Begg *et al.* 1994; Greenway *et al.* 2006). Two further processes affect the chemistry of the rice rhizosphere (Fig. 1, Processes 3 and 4): oxidation of inorganic reductants, such as ferrous iron, by O_2 from the roots and associated generation of H^+ (Begg *et al.* 1994; Kirk & Bajita 1995); and release of H^+ from the roots to balance excess intake of cations (particularly NH_4^+) over anions. These inputs of H^+ will tend to offset H^+ consumption in venting of dissolved CO_2 from the soil and the resulting changes in carbonate equilibria.

Changes in dissolved CO_2 and pH potentially affect Zn stress in two ways. First, by alleviating bicarbonate (HCO_3^-) toxicity to the roots, which is associated with the large dissolved CO_2 concentrations, the soil pH being buffered near neutral in most submerged soils so that the concentration of HCO_3^- exceeds that of dissolved CO_2 (note $pK_1 = 6.4$ where K_1 is the apparent first dissociation constant of H_2CO_3) (Ponnamperuma 1972; Kirk 2004). Large HCO_3^- concentrations cause oxidative stress to the roots by forming radical oxygen species (ROS), and this is exacerbated under Zn deficiency, particularly in sensitive genotypes, because ROS-scavenging superoxide dismutase enzymes contain and require Zn (Hacisalihoglu & Kochian 2003; Rose *et al.* 2011, 2012).

Second, removal of CO_2 will cause the rhizosphere pH to increase, leading to dissolution of Zn-complexing organic ligands from soil organic matter and hence solubilisation of Zn in the soil solid (Fig. 1, Processes 6 and 7). At pHs near neutral, this effect may dominate other processes affecting the solid-solution distribution of Zn, such as pH-dependent precipitation-dissolution of Zn carbonates (references in Discussion). Therefore Zn uptake by the roots will increase. These two sets of effects (decreased HCO_3^- toxicity and increased Zn solubility) may act together or separately. Further, there may be genotype differences in the extent of CO_2 venting, and the extent of venting will increase with increasing planting density, consistent with the observed beneficial effect of planting density on Zn stress. However this is not well quantified or understood.

In this article we investigate CO_2 uptake by rice roots growing in submerged soil and the associated changes in rhizosphere chemistry affecting Zn solubility and HCO_3^- toxicity, and the extent to which these effects can explain genotype differences in Zn deficiency tolerance and the observed effect of planting density on Zn stress.

MATERIALS AND METHODS

Plant growth

We planted 4-wk (week) old rice seedlings into a flooded, strongly-reduced, Zn-deficient rice soil at either 1 or 4 plants per container, planted closely together, and followed changes in soil solution chemistry and plant growth. The details follow.

We used the same soil as in our earlier field experiment (Mori *et al.* 2016). It is a Hydraquent (USDA Soil Taxonomy) from rice fields at Tiaong, Quezon Province, Philippines. Portions of topsoil (0-30 cm depth) were air dried and sieved (< 2 mm). The properties of the sieved soil were 42% clay, 40% silt, pH (aerobic in H_2O) 8.5, CEC 90 $mmol_c$ kg^{-1}, organic C content 73 g kg^{-1} and carbonate content 96 g kg^{-1}. The available Zn content of the flooded soil at transplanting (determined by isotopic exchange) was 2.3 mg kg^{-1} and the total soil Zn content (determined by acid digestion) was 83.2 mg kg^{-1} (Izquierdo *et al.* 2016).

Portions (1.2 kg) of the air dried soil were mixed with 0.3 g kg^{-1} of N as urea and 10 g kg^{-1} of rice straw, to stimulate anaerobic reduction processes, and then saturated with deionized water to make a slurry. The slurry was poured into 10-cm by 8-cm, 21-cm deep glass containers to a depth of 18.5 cm. We used glass containers to ensure there was no entry of O_2 into the reduced soil through the sides. Each container was fitted with three rhizon solution samplers (Rhizosphere research products, Wageningen, Netherlands) with a 5-cm porous section, and fitted with Luer locks. The samplers were held vertically in the soil so that the porous section ran from 8.5 to 13.5 cm below the floodwater-soil boundary, and at 0.5, 1.5 and 3 cm from the middle of the containers along the longer axis. Further deionized water was added to bring the level to the top of the containers, and the water standing in the containers was maintained at this level through the experiment. The resulting bulk density was 0.81

kg dm^{-3} and the volumetric water content 0.69. The soil was allowed to become reduced for 28 d at 30 ^{o}C before transplanting the rice seedlings.

Seeds of Zn-deficiency tolerant (IR55179-3B-11-3, hereafter IR55179) and sensitive (IR26) rice genotypes were germinated in petri dishes at 30 ˚C in complete darkness for 3 d (days). These genotypes differ in their growth and Zn uptake under Zn-deficient conditions but have similar growth when Zn is non-limiting (Mori *et al.* 2016). The germinated seeds were transferred to a mesh floating on Zn-free Yoshida nutrient solution (Yoshida *et al.* 1976), and grown for 28 d before being transplanted manually into the pre-reduced soil in the containers. The seedlings were placed with the root crown at approx. 5 cm below the soil-floodwater boundary, as is the practice for growing rice in this soil in the field because of its loose structure and hence weak support for seedlings (Mori *et al.* 2016). Three replicates were made for each of the two genotypes and two planting densities. The planted containers were arranged in a random order and the plants were grown for 33 d. The growth conditions – both before and after transplanting – were 13.5 h light (600 μmol m^{-2} s^{-1} white light) at 30 ˚C and 10.5 h dark at 24 ˚C.

At weekly intervals, in both the planted and unplanted containers, soil solution was withdrawn from each of the three rhizon samplers per container (at 0.5, 1.5 and 3 cm from the middle of the containers as described above), into pre-evacuated 2-cm^{3} vials, and analysed for dissolved CO_2, pH, major cations and anions, and Zn by the methods described below. Also at weekly intervals, redox potential (E_H) was measured using a probe (HI1297D , Hanna Instruments, Rhodes Island, USA) inserted into the soil to 8-cm depth, 3-cm from the middle on the opposite side to the solution samplers. At 33 d after transplanting, the aerial plant parts were separated from roots at the root crown limit. The fresh biomass was measured and the roots and shoots were then thoroughly washed with deionized water and dried at 70 ˚C for 5 d.

In separate replicate, unplanted containers, the composition of gas bubbles accumulated in the soil was measured by periodically fitting over each container a 3 dm^{3} gas-tight bag fitted with a sampling port, and agitating the containers to displace entrapped soil gases into the headspace. Samples of the headspace were withdrawn by syringe and analysed for CO_2 and CH_4 by gas chromatography (Cambridge Scientific Instruments 200 Series GC with thermal conductivity detector).

Plant analysis

The dry plant material was ground with a micro hammer-mill grinder (Culatti AG, Zurich, Switzerland) and the ground material digested in concentrated, analytical grade HNO_3 and H_2O_2 in a microwave digestion system (MARSXpress, CEM Corporation, Mathews, NC, USA). The extracts were analysed for Ca, Mg, Fe, Mn, K, P, S, Cl and Zn by ICP-MS (PerkinElmer NexION 350, Boston, MA, USA) and N by an elemental analyser (Vario EL III Elementar Analyser, Langenselbold, Germany). Root Zn concentrations could not be reliably determined because of interference from soil material adhering to root surfaces. This is a particular problem in puddled, flooded, clayey soils of the sort in our experiment, and we know of no reliable way of dealing with it (discussed further by Mori *et al.*, 2016). We calculated total Zn uptake by assuming root Zn concentration was equal to shoot Zn concentration.

Soil solution analysis

The solutions were analysed for dissolved CO_2 (MI-720 electrode, Microelectrodes Inc, USA) and pH (MI-410 combination electrode, Microelectrodes Inc, USA) within 30 min of sampling. The CO_2 electrode was calibrated using freshly prepared $NaHCO_3$ solutions of known concentrations in sealed 12.5 cm^3 vials and buffered at pH 3 by addition of oxalic acid so that all the added carbonate was converted to dissolved CO_2. Concentrations of HCO_3^- were calculated from the measured dissolved CO_2 and pH using $[HCO_3^-] = [H_2CO_3^*]/(K_1[H^+])$ where $[H_2CO_3^*] = [CO_2] + [H_2CO_3] \approx [CO_2]$ and K_1 is the apparent first dissociation constant of H_2CO_3, adjusted for ionic strength (using the Davies equation).

The concentrations of Ca, Mg, Fe, Mn, K, S and Cl were analysed by ICP-MS (PerkinElmer NexION 350, Boston, MA, USA). The concentrations of Zn were determined using isotope dilution mass spectroscopy. The analytical details are given in Appendix 1. In brief, the soil solution is spiked with the isotope ^{67}Zn, the spiked solution is passed through anion exchange columns to remove interfering ions, and the isotope composition of the resulting solution measured. The Zn concentration in the original solution is then found using the isotope composition to correct for any losses in the

purification process. Speciation and precipitation calculations were made using MINTEQ (Gustaffson 2012).

Soil acid-base changes

The acidity consumed in CO_2 venting was found from the decrease in HCO_3^- in the soil solution, summed over the whole soil volume. Note that (a) a water-saturated soil is effectively a closed system, so CO_2 venting through the roots shifts the equilibrium $HCO_3^- + H^+ = CO_2 + H_2O$ to the right; (b) $[CO_3^{2-}]$ is negligible at the pHs of our experiments ($pK_2 = 10.3$ where K_2 is the second dissociation constant of H_2CO_3); and (c) additional CO_2 formed from the turnover of root-derived substrates and lost from the soil, does not cause additional net changes in soil acidity. The acidity released from roots to balance the plant cation and anion intake was found, following Begg *et al*. (1994), from the equivalents of the major cations (NH_4^+, K^+, Ca^{2+}, Mg^{2+}) and anions (Cl^-, H_2PO4^-, SO_4^{2-}) taken up. Protons are also produced in the oxidation and subsequent hydrolysis of inorganic reductants, such as ferrous iron (Fe^{2+}), by root-released O_2 (Fig. 1). But, based on the composition of the soil solution (Results), the concentration of Fe^{2+} in our reduced soil was far smaller than the concentration of HCO_3^-. So this source of acidity was probably small.

Mathematical model of Zn uptake

We developed a model with which to test the null hypothesis that the effects of planting density and genotype on uptake do not depend on plant-induced solubilisation of soil Zn. The model calculates the largest possible uptake of Zn for the measured root density if the roots act as sinks for Zn but do not otherwise influence the soil Zn solubility. By comparing the predictions of the model, made using independently-measured parameter values, with our observed rates of uptake, we could conclude whether or not solubilisation is taking place.

Full descriptions of the model and its parameterisation are given in Appendices 2 and 3. The model is based on that of Baldwin *et al*. (1973), which starts from the assumption that the concentration profile of a solute being absorbed around a root is given by the steady-state equation

$$I = 2\pi\alpha a C_{La} = 2\pi r\, Db\, \frac{dC_L}{dr} \tag{1}$$

where I is the inflow per unit root length, α is the root absorbing power (defined by this relation), a is the root radius, C_{La} is the concentration in solution at the root surface, r is radial distance, D is the diffusion coefficient and b the buffer power (dC/dC_L where C is the concentration in the whole soil). The soil diffusion coefficient is given by

$$D = D_L \theta f / b \tag{2}$$

where θ is the soil volumetric water content and f is a diffusion impedance factor. Each root is assigned a cylinder of depletion of radius x, which spreads out until it meets the depletion zone around neighbouring roots:

$$x = a + 2\sqrt{Dt} \text{ until } a + 2\sqrt{Dt} > 1 / \sqrt{\pi L_V} \tag{3}$$

where L_V is the root length density. From these relations the following equation is obtained for uptake when $\alpha a \gg Db$ (i.e. the rate limiting step is diffusion through the soil, not the uptake across the root surface – see Appendix 3 for evidence from measured uptake kinetics that this condition is satisfied in our system):

$$\Delta M_t = M_t \left[1 - \exp\left\{ \frac{2\pi\, DL_V \Delta t}{0.5 + \frac{x^2}{x^2 - a^2}\ln\frac{a}{x}} \right\} \right] \tag{4}$$

where ΔM_t is the amount absorbed over time interval Δt and M_t is the amount in the soil at time t.

To implement the model, we divide the roots into $k = 3$ size classes (diameters < 0.1, 0.1–0.4 and > 0.4 mm) and calculate the length of each size class on daily time steps over the course of our experiment using relationships obtained by Mori *et al.* (2016) for our genotypes, soil and growth conditions, as follows:

(a) the total root FW at each time step (W_i) is calculated from the measured root FW at the start and end of the experiment assuming exponential growth;

(b) the proportion of total root FW in each size class at each time step (P_{ik}) is found from Mori *et al.*'s data for P_k versus time, and the FW of each size class is calculated from $W_{ik} = P_{ik} \times W_i$. The length of new root formed in each size class at each time step is then found from

$$\Delta L_{ik} = \left(W_{ik} - W_{i-1,k}\right) / \left(\rho \pi a_k{}^2\right) \tag{5}$$

where a_k is the mean root radius of the class (obtained from Mori *et al.*'s data) and ρ is the root tissue density (= 1 g FW cm^{-3}, Birouste *et al.* 2014). We then calculate the uptake by each root (length $L_{ik} = L_{i-1k} + \Delta L_{ik}$) from the day it is formed onwards using Eqn (4) with daily time steps:

$$\Delta M_{ik} = M_i \left[1 - \exp \left\{ \frac{2\pi \, DL_{Vik} \Delta t}{0.5 + \dfrac{x_{ik}{}^2}{x_{ik}{}^2 - a_k{}^2} \ln \dfrac{a_k}{x_{ik}}} \right\} \right] \tag{6}$$

where $L_{Vik} = L_{ik} / \text{vol}$, where vol is the whole soil volume, and x_{ik} is the width of the depletion zone calculated for each root class and age with Eqn (3). The total uptake is the sum of the uptakes by individual roots over time.

Data analysis

Statistical analyses were made using the Agricolae package of the R Project (de Mendiburu 2016). Two-way ANOVA was used to determine the significance of genotype and planting density effects, with repeated measures for the time-course data. Differences between means were analysed using *post hoc* Fisher Least Significant Difference.

RESULTS

Plant growth

Total shoot and root growth per contained increased with planting density in both genotypes and were greater in IR55179 than IR26 at both planting densities (Fig. 2a,b). This is consistent with our previous findings (Mori *et al.* 2016). The root:shoot ratio did not differ between the genotypes at the smaller planting density, and was smaller in IR26 at the larger planting density but not in IR55179

(Fig. 2c). In both genotypes, at the smaller planting density, shoot Zn concentration was at or close to the critical value for deficiency (20 µg g^{-1} – Dobermann & Fairhurst 2000), but at the larger planting density, it was well above the critical value, and more so in IR55179 (Fig. 2d). Total plant Zn uptake per container also increased with planting density, roughly in proportion to the number of plants; at both densities uptake per container in IR55179 was more than double that in IR26 (Fig. 2e). Uptake per plant was far greater in IR55179 at both planting densities (Fig. 2f), and increased with planting density in IR55179, though to a smaller extent than in Mori *et al*.'s (2016) field experiment. We propose this was because the volume of soil available to the roots was smaller than in the field experiment and depletion of soil Zn was correspondingly greater. The uptake of Zn by IR55179 at 4 plants container^{-1} (434 µg container^{-1}) corresponds to a depletion of 16% of the readily plant-available Zn (= 2.3 µg g^{-1} × 1,200 g container^{-1} = 2,760 µg container^{-1}).

Figure 3 shows the concentrations of macronutrients in the plant shoots. In all cases these were well above critical values for deficiency in rice during vegetative growth (25, 15, 1, 1.1, 1.5 and 1.3 mg g^{-1} for N, K, P, S, Ca and Mg, respectively – Dobermann & Fairhurst 2000). The concentrations of all the macronutrients except Ca were smaller in IR55179 at both planting densities, and in both genotypes at the higher planting density, presumably because greater growth resulted in dilution of these nutrients. This is in contrast to shoot Zn concentrations, which were greater in IR55179 and in both genotypes at the higher planting density (Fig. 2d). The ratio of the concentration of Zn to that of P, which, like Zn, has low mobility in the soil, doubled with increase in planting density in both genotypes. The difference in uptake per plant (i.e. concentration × plant DW per plant) between IR55179 at high planting density and IR26 at low density relative to the latter was from -0.41 to 0.32 for the macronutrients (-0.41, 0.07, -0.18, -0.20, 0.32 and 0.15 for N, K, P, S, Ca and Mg, respectively) but 2.11 for Zn. That Zn behaves very differently to the macronutrients is good evidence for a tolerance mechanism or mechanisms specifically affecting Zn.

Figure 3 also shows the shoot concentrations of Fe and Mn. These were well above critical values for deficiency (70 and 40 µg g^{-1}, respectively – Dobermann & Fairhurst 2000) but below toxic levels (300–500 and 800–2,500 µg g^{-1}, respectively – ibid). Shoot concentrations of Mn and to a lesser extent Fe were greater at the higher planting density, although concentrations of both in the soil

solution were less (next section). The shoot Fe and Mn concentrations were an order of magnitude greater than shoot Zn concentrations, and the soil solution concentrations two orders of magnitude greater than soil solution Zn.

Soil solution composition

Figure 4 shows the time courses of dissolved CO_2, pH, E_H, calcium (Ca), magnesium (Mg) and bicarbonate (HCO_3^-) in the soil solution. There were no significant differences ($P < 0.05$) in these variables between the three soil solution samplers in each container at any time except at the first sampling time. The values shown in Fig. 4 are averages across the three samplers. The concentrations of other elements (Fe, Mn, K, Na, N, P, S, Cl) were less than 0.2 mM (Appendix 4).

Figure 4 shows that the concentration of dissolved CO_2 was roughly constant in the unplanted soil (5.1 to 4.9 mM between -17 and 26 d from transplanting – equivalent CO_2 partial pressure approx. 15 kPa), whereas the E_H decreased (-208 to -224 mV over same period) and pH and HCO_3^- concentration increased (6.9 to 7.2 and 24 to 39 mM, respectively). The concentrations of Ca and to a greater extent Mg also decreased in the unplanted soil over the course of the experiment (1.5-fold and 2.4-fold, respectively). Small (< 1 mm diameter) entrapped gas bubbles were visible in the soil, which on displacement (Materials and Methods) were found to be a mixture of CO_2 and CH_4 with CH_4/CO_2 ratio 1.4 at 10 d after flooding the soil and increasing approximately linearly to 3.4 at the end of the experiment, with little effect of the plants on this ratio (data not shown). Note CH_4 is 26 times more volatile than CO_2 (Henry's law constants 1.29×10^{-5} and 3.39×10^{-4} M kPa^{-1}, respectively – Stumm & Morgan 1996), so the fact that these ratios were less than 26 implies greater rates of CO_2 production than CH_4.

The observed changes are typical of carbonate containing soils following submergence (Ponnamperuma 1972). Immediately after submergence, the pH falls as CO_2 and organic acids formed in oxic and then anoxic respiration, accumulate in the soil. Continuing redox reactions in the anoxic soil consume protons (reduction of NO_3^-, Mn(IV), Fe(III) and SO_4^{2-}), so the decrease in pH is gradually reversed. There is then a gradual re-precipitation of carbonates, though subject to inhibition by dissolved organic compounds and other factors (e.g. Kirk *et al.* 2015). Calculations with the

MINTEQ equilibrium speciation model (Gustaffson 2012) show that the soil solution in the unplanted soil was saturated with respect to calcite ($CaCO_3$), magnesite ($MgCO_3$) and dolomite ($CaMg(CO_3)_2$) throughout the experiment. Likewise there were gradual decreases in Fe and Mn in solution (Figure S1), consistent with precipitation of mixed carbonates.

The growth of the plants greatly altered these relations (Fig. 4). After the initial period, the dissolved CO_2 concentration at the greater planting density was less than in the unplanted controls, and more so in IR55179 than IR26 (Fig. 4a). The soil pH values roughly mirrored the changes in dissolved CO_2, tending to increase as the dissolved CO_2 decreased (Fig. 4b). There were also increases in E_H at the higher planting density (Fig. 4c), presumably due to release of O_2 from the roots brought down through the root aerenchyma. Consistent with this, the concentrations of Fe and Mn in solution decreased, and the concentrations of S increased, consistent with oxidation of Fe(II) and Mn(II) to insoluble Fe(III) and Mn(IV) oxides, and S(-II) to more-soluble SO_4^{2-} (Appendix 4).

The changes in dissolved CO_2 concentration compared with the unplanted controls reflect rates of CO_2 generation in the soil from root-derived carbon (soluble exudates, insoluble secretions, detrital matter), versus rates of loss by venting through the roots. Both of these are expected to be greater at the greater planting density. Evidently, rates of CO_2 venting increased more than rates of generation in IR55179 because there was greater depletion of soil CO_2 (Fig. 4a). In IR26, rates of CO_2 generation increased around the middle of the experiment, presumably because there was greater release of organic substrates from the roots. This is expected with impaired membrane integrity under Zn stress in less tolerant genotypes (Rose *et al.* 2011). The subsequent dip in dissolved CO_2 (and increase in E_H) may indicate recovery of root growth once the plants had accumulated sufficient Zn. In both genotypes at the higher plant density, dissolved CO_2 increased at the last sampling: we presume that was because by this stage the roots were becoming container-bound.

The changes in soil pH reflect H^+ consumption in removal of dissolved CO_2 and carbonate species by venting through the roots, tending to raise the pH; versus H^+ release from roots to balance excess intake of cations over anions, tending to lower the pH (next section). The changes in HCO_3^- concentration (Fig. 4f) reflect the changes in dissolved CO_2 and pH. Hence, after the initial stages, the HCO_3^- concentration was smaller at the greater planting density, and especially so in IR55179. The

decreases in Ca and Mg in solution (Fig 4d,e) reflect (a) the decreases in HCO_3^-, it being the main anion balancing cations in solution; and (b) increases in the soil surface negative charge with increased pH, and associated increased cation sorption on soil surfaces.

Soil acid-base changes

Figure 5 shows the observed changes in $[CO_2]$, pH and soil acidity compared with the unplanted controls at 26 d after transplanting, when CO_2 venting from the soil was greatest. The acidity released to balance cation-anion intake reflects the plant biomass and its composition. Although the plant biomass was much greater at higher planting density (Fig. 2), because of nutrient dilution (Fig. 3) the acidity released was not much greater (Fig. 5c). Figure 5 shows the pH changes caused by the plants were mainly related to the changes in HCO_3^- caused by CO_2 venting.

Figure 5d gives the changes in CO_2 compared with the unplanted controls, relative to root mass. It shows the differences in root mass (> two-fold between the genotypes at the higher planting density) may in part explain differences in venting between the genotypes.

Zinc concentration in the soil solution

Figure 6 shows the time courses of Zn in the soil solution. The concentrations are close to the detection limits ($c.$ 0.01 μM), and this is reflected in the large error bars. In all the treatments, the concentration decreased over time, including in the unplanted soil, presumably due to continuing slow immobilization reactions with the soil solid. The concentrations did not differ greatly between the treatments, in spite of the much greater removal of Zn from the soil at the higher planting densities.

Calculations with the MINTEQ model (Gustaffson 2012) indicate that the soil solution Zn concentrations were not controlled by any of the well-characterised Zn carbonate minerals. But the solutions were saturated with respect to $MgCO_3$ and $CaMg(CO_3)_2$ and calculations show a Mg-Zn carbonate solid solution could have formed (Appendix 5). Reductive dissolution of solid phases following soil submergence favours co-precipitation in solid solutions, and because Zn^{2+} and Mg^{2+} have similar lattice ionic radii (0.074 and 0.072 nm, respectively), Zn^{2+} may substitute for Mg^{2+} in Mg carbonate lattices. The soil solutions were also saturated with respect to the Zn sulphide mineral

sphalerite (ZnS), so this may also have been present. Irrespective of what solid phases control Zn in solution, their dissolution would be sensitive to changes in CO_2 concentration and pH (Discussion).

Relation between shoot Zn concentration and dissolved CO_2

Figure 7 shows a near linear inverse relation between the shoot Zn concentration and dissolved CO_2 in the two genotypes at the two planting densities.

Predicted Zn uptake

Figure 8a gives the predicted uptake by the model and the measured uptake at 33 d after transplanting. The predictions were made using parameter values that were all measured or estimated independent of the measured uptake (Materials and Methods and Appendix 3). For IR26 the agreement between observed and predicted uptake is good at the lower planting density but poor at the higher density, and for IR55179 it is poor at both planting densities and very poor at the higher density. Figure 8b shows the model predictions with the same set of parameter values except for the concentration of readily plant-available Zn which is increased by the factors indicated so as to obtain good agreement with the observed uptake.

The sensitivity of predictions to key model parameters is shown in Fig. 8c. The predictions are very sensitive to increases in the concentration of plant-available Zn, and to a lesser extent, to the proportion of root FW as fine roots. For IR55179 at 4 plants container^{-1}, the measured uptake is predicted with 2.75 times the measured plant-available Zn, but the proportion of fine roots must be multiplied by 7.5 to match observed uptake. The predictions are also sensitive to the soil Zn buffer power, b (Eqn 2). A 4-times decrease in b (i.e. a 4-times increase in the Zn concentration in the soil solution for a given level of plant-available Zn) gives good agreement with the observed uptake.

DISCUSSION

The observed genotype and planting density effects on Zn uptake were both associated with decreases in dissolved CO_2 in the rhizosphere due to CO_2 venting through the roots. In the discussion that follows we show that decreases in dissolved CO_2 and associated increases in soil pH are expected to

cause solubilisation of Zn and thereby increased plant Zn uptake. This mechanism can explain, at least in part, rice genotype differences in tolerance of Zn deficiency.

The experimental evidence

Genotype differences in Zn uptake may be due to inherent differences in root growth or differences in internal use efficiency or external uptake efficiency, or a combination of all three. Better root growth as a result of better Zn uptake will in turn produce more Zn uptake, so small changes in internal or external efficiency can have large cumulative effects on uptake (Wissuwa 2003). Past work has shown that maintenance of root growth under Zn stress is at least a part of genotype differences (Widodo *et al.* 2010; Rose *et al.* 2013; Nanda & Wissuwa 2016). Differences in growth are apparent almost immediately after transplanting contrasting genotypes into Zn deficient soil, well before there are large differences in uptake (Nanda & Wissuwa 2016). Mori *et al.* (2016) showed in Zn-free nutrient culture that tolerant genotypes had better root development, and since no additional Zn could have been taken up, the better growth must have been due to better internal use of the Zn, including in re-translocation of shoot Zn into the roots. Internal tolerance of HCO_3^- stress linked to Zn deficiency is also part of genotype differences (Rose *et al.* 2011, 2012). However these internal mechanisms cannot by themselves account for the planting density effect which necessarily involves external processes.

The large dissolved CO_2 concentrations we measured are typical of many flooded soils because CO_2 formed in soil respiration escapes only slowly through water-filled soil pores (Introduction). Degassing of dissolved CO_2 into the root aerenchyma followed by diffusion to the atmosphere provides an easier exit route. Evidently the tolerant genotype at high planning density provided more-efficient root venting. Greater root growth should mean a larger conduit for venting via the root aerenchyma. It will also mean more deposition of substrates into the rhizosphere fuelling CO_2 generation in soil respiration, as well as more CO_2 from root respiration. Zinc-deficiency tolerant genotypes leak less substrates from their roots under low Zn and high HCO_3^- stress (Rose *et al.* 2011, 2012), including our tolerant genotype IR55179 compared with the intolerant IR26 (Lee *et al.* 2017a), and this may offset the greater deposition expected with the several-fold greater root growth of IR55179 at high density. A complete assessment of genotype differences in venting would need to

consider (a) differences in rhizodeposition; (b) differences in aerenchyma and root porosity (porosities of lowland rice genotypes range between 30 and 40% under given anoxic growth conditions – Colmer 2003; Wissuwa unpublished); (c) barriers to gas transfer in root walls (Colmer 2003); (d) other differences in root anatomy, especially the proportions of aerenchymatous primary roots versus non-aerenchymatous fine laterals (Kirk 2003); and (e) differences in enzymatically-mediated degassing of dissolved CO_2 (see Implications for gene mapping and plant breeding).

The modelling evidence

The purpose of the modelling was to test how far the measured uptake could be explained without allowing for Zn solubilisation by CO_2 venting or other root-induced changes in the soil. The model is based on the null hypothesis that the roots behave as sinks for Zn but do not otherwise influence its solubility in the soil, and the assumption that the root Zn-absorbing properties are non-limiting, i.e. αa $>> Db$. This assumption is shown to be justified in Appendix 3 by evaluating αa using published data for the kinetics of Zn uptake by -affinity root transporters under the very low soil solution concentrations of our system.

With the standard set of input parameters, the model predicts the observed uptake well for the intolerant genotype at the low planting density. But it under-predicts uptake at the higher planting density and for the tolerant genotype at both planting densities. Evidently, uptake rates were enhanced in some way that the model or the parameter values used do not adequately account for. Given that the root Zn absorbing properties were non-limiting in the model, this cannot be because of better root absorbing properties, such as through more active membrane transport systems. It must either be due to a greater root absorbing surface, or some root-induced change in the soil that makes the soil Zn more soluble.

Good agreement between observed and predicted uptake was achieved for both genotypes and planting densities by increasing the modelled concentration of plant-available Zn in the soil, i.e. by simulating a process causing solubilisation of Zn. The required multiplier of plant-available Zn is greater for the tolerant genotype and the higher planting density. This is consistent with greater root-induced solubilisation of Zn by the tolerant genotype, and an amplified effect at the higher planting

density. Both of these are consistent with the observed greater depletion of CO_2 by the tolerant genotype and at the higher planting density, if the soil Zn solubility is linked to carbonate equilibria. We discuss why this should be the case in Effects of CO_2 venting on soil Zn solubility.

Increased uptake might also be due to a greater proportion of root FW being in fine roots, fine roots having a greater length per unit root FW. However, the predicted uptake is less sensitive to the proportion of fine roots than to the concentration of plant-available Zn, and a larger multiple of the proportion of fine-roots is needed to obtain agreement with the observed uptake. Further, there is no obvious reason why the proportions of fine roots should be much greater than we have assumed based on Mori *et al*. (2016) data for the genotypes and growth conditions in our experiment, and why they should increase with increased planting density. Whereas there are good reasons to expect increased Zn solubilisation and uptake with greater CO_2 venting (next section).

Good agreement between the observed and predicted uptake is also achieved by decreasing the soil Zn buffer power, which is equivalent to increasing the Zn concentration in the soil solution, C_L, for a given concentration of plant-available Zn. However there is no reason to think our measurements underestimate C_L to the extent required. If anything we may have over-estimated C_L at the very small values we are concerned with.

Zinc solubilised by a root may diffuse away from the root as well as towards it, and the fraction taken up will depend on the spread of the solubilising agent away from the root and the interception by neighbouring roots, which will depend on rooting density. Increased rooting density therefore has two benefits: it means the solubilising agent is concentrated in the region between neighbouring roots and so its solubilising effect is amplified, and also the fraction of solubilised Zn taken up is increased.

Effect of CO_2 venting on soil Zn solubility

By *soluble* Zn we mean those forms of soil Zn that are in rapid equilibrium with the soil solution and therefore freely-available for uptake by roots. The bulk of the soil Zn is in forms that are only sparingly-soluble and only slowly equilibrate with the soil solution. Processes affecting Zn solubility (i.e. the concentration of soluble forms) include complexation-decomplexation reactions in the soil solution, adsorption-desorption reactions with the soil solid, and precipitation-dissolution reactions.

The modelling results suggest the tolerant genotype at the higher planting density caused an approximately two-fold increase in Zn solubility. Conceivably, increases in E_H caused by root-released O_2 resulted in dissolution of Zn associated with soil reductants. However this can only have been a small effect because the concentrations of potential reductants in the soil – Mn(II), Fe(II), S(-II) – were small (< 0.2 mM in the soil solution, Appendix 4); far smaller than the concentrations of carbonates. Solubilisation through CO_2 venting is a more plausible explanation according to the following reasoning.

Venting of CO_2 induces the following changes.

(1) The equilibrium $HCO_3^- + H^+ = CO_2 + H_2O$ is shifted to the right resulting in a decrease in HCO_3^- in the soil solution and increase in pH.

(2) The increase in pH is buffered by rapid exchange reactions with proton-donating groups in the soil solid:

$$\text{soil–H} + M^+ = \text{soil–M} + H^+ \tag{7}$$

where soil–H represents a proton donating group – mainly, in our soil, carboxylic and phenolic groups in soil organic matter (the soil contains 73 g kg^{-1} organic C) and M^+ is an exchangeable cation – mainly Ca^{2+} and Mg^{2+} (the soil contains 66 g kg^{-1} Ca + Mg carbonates).

(3) Processes (1) and (2) together mean Ca^{2+} and Mg^{2+} in the soil solution decrease (at the higher planting density they decreased approx. 0.5-fold) and therefore the saturation indices of Ca and Mg carbonates decrease; however in all our treatments the solution remained saturated with respect to $CaCO_3$, $MgCO_3$ and $CaMg(CO_3)_2$.

(4) However, because organic matter becomes more soluble with increased pH as dissociation increases the negative charge on organic surfaces (Eqn 7), the concentrations of metal-complexing organic ligands in solution increase, resulting in solubilisation of Zn.

The Zn^{2+} ion has a strong affinity for organic ligands. So the increased solubility of organic matter at higher pH should be expected to decrease the concentration of free Zn^{2+} in solution and thereby increase dissolution of Zn in carbonates or other solid phases, i.e. the plant-available Zn will increase. Increases in Zn solubility in acid soils adjusted above pH 7.0 have been observed in previous studies

and attributed to solubilisation by organic ligands (Saeed & Fox 1977; McBride & Blasiak 1979; Brümmer *et al.* 1983). The decreases in acidity shown in Fig. 5c are of the order of 10 $mmol_c$ kg^{-1}. This is more than two orders of magnitude greater than the available Zn content of the unplanted soil. Hence a two-fold increase in plant-available Zn by this mechanism is realistic.

Implications for gene mapping and plant breeding

Our experimental soil has the characteristics most often associated with Zn deficiency in rice in the field: it is young with weak profile development, it is perennially wet, it has a large organic carbon content, and it contains free carbonates (van Breemen *et al.* 1980; Impa & Johnson-Beebout 2012). The Zn deficiency in this type of soil, due to low Zn solubility, is more widespread that the type associated with low total Zn content (Impa & Johnson-Beebout 2012), and is the appropriate target for plant breeding. The mechanisms suggested by our results are likely to hold in other rice soils with this type of Zn-deficiency.

Conventional QTL mapping and GWAS analysis to identify markers for Zn deficiency tolerance indicate it is a complex trait with multiple causative mechanisms and associated genes (Widodo *et al.* 2010; Lee *et al.* 2017b). Progress in gene mapping will require genes for specific traits to be identified. What traits might lead to enhanced CO_2 venting? Differences in root architecture and gas permeability may be involved (discussed in The experimental evidence), but it may be difficult to identify markers for root architecture traits. The possible role of the enzyme carbonic anhydrase (CA) in degassing dissolved CO_2 from the root apoplast into aerenchyma, is interesting. It may be significant that the active site of most CAs contains Zn and CA activity in rice leaves is suppressed under Zn deficiency (Sasaki *et al.* 1998). Xu *et al.* (2007) found that expression of the gene OsCA1, which mediates CA activity, was enhanced in a Zn-deficiency tolerant genotype (Nipponbare) exposed to HCO_3^- stress, resulting in increased CA activity. A further possibility is that tolerant genotypes have Zn-independent CA, as found by Lane *et al.* (2005) in a marine diatom adapted to low-Zn waters.

Would enhanced CO_2 venting through roots also mean greater emissions of the greenhouse gas methane (CH_4)? Rice roots can act as conduits for CH_4 venting from the soil, as well as fuelling CH_4

formation by providing substrates through exudates and debris (references in Kirk 2004). However they are also sources of O_2 and part of the CH_4 is oxidized en route through the rhizosphere and aerenchyma (references in Kirk 2004). Arah and Kirk (2000) showed with a model of rice plant-mediated CH_4 emission that genotypes with high specific root transmissivity may, other things being equal, reduce rather than enhance net emission. Also less leakage of carbon substrates from roots under improved Zn nutrition will mean less CH_4 formation (van der Gon *et al.* 2002).

CONCLUSIONS

1   The observed differences in Zn uptake between rice genotypes and planting densities were at least in part due to root-induced changes in the soil making Zn more soluble. While genotype differences in solubilisation of Zn and other micronutrients are well established for other plant species, they are not well established for rice in flooded soil.

2   A plausible mechanism for this solubilisation, consistent with our results, is increased venting of CO_2 from the soil solution through the roots, resulting in increases in soil pH. Increases in pH in the range in our system are expected solubilise Zn by dissolution of alkali-soluble, Zn-complexing organic ligands from soil organic matter.

3   Greater planting density would both concentrate the Zn solubilising effect of CO_2 venting and increase the fraction of Zn solubilised taken up. Hence our experimental observations are explained by this mechanism.

4   Differences in venting of soil CO_2 through roots are a valid new target for rice breeding for Zn-deficiency tolerance. Methods for measuring genotype differences in venting need to be developed, appropriate for the root anatomical or biochemical traits involved.

ACKNOWLEDGMENTS

Government's Department for International Development (DFID) and the Bill & Melinda Gates Foundation.

REFERENCES

Arah J.R.M. & Kirk G.J.D. (2000) Modelling rice plant-mediated methane emission. *Nutrient Cycling in Agro-Ecosystems* 58, 221–230.

Arnold T., Kirk G.J.D., Wissuwa W., Frei M., Zhao F.-J., Mason T.F.D. & Weiss D.J. (2010) Evidence for the mechanisms of zinc uptake by rice using isotope fractionation. *Plant, Cell & Environment* 33, 370–381.

Baldwin J.P., Nye P.H. & Tinker P.B. (1973) Uptake of solutes by multiple root systems from soil. III. A model for calculating the solute uptake by a randomly dispersed root system developing in a finite volume of soil. *Plant & Soil* 38, 621–635.

Begg C.B.M., Kirk G.J.D., MacKenzie A.F. & Neue H.-U. (1994) Root-induced iron oxidation and pH changes in the lowland rice rhizosphere. *New Phytologist* 128, 469–477.

Birouste M., Zamora-Ledezma E., Bossard C., Pérez-Ramos I.M. & Roumet C. (2014) Measurement of fine root tissue density: a comparison of three methods reveals the potential of root dry matter content. *Plant and Soil* 374, 299–313.

Brümmer G., Tiller K.G., Herms U. & Clayton P.M. (1983) Adsorption-desorption and/or precipitation-dissolution processes of zinc in soils. *Geoderma* 31, 337–354.

Colmer T.D. (2003) Aerenchyma and an inducible barrier to radial oxygen loss facilitate root aeration in upland, paddy and deep-water rice (*Oryza sativa* L.). *Annals of Botany* 91, 301–309.

de Mendiburu F. (2016) *Agricolae: Statistical procedures for agricultural research.* http://tarwi.lamolina.edu.pe/~fmendiburu.

Dobermann A. & Fairhurst T. (2000) *Rice nutrient disorders and nutrient management*. Potash and Phosphate Institute, Singapore and International Rice Research Institute, Manila.

Greenway H., Armstrong W. & Colmer T.D. (2006) Conditions leading to high CO_2 (>5 kPa) in waterlogged–flooded soils and possible effects on root growth and metabolism. *Annals of Botany* 98, 9–32.

Gustafsson J.P. (2012) *Visual MINTEQ Version 3.0*. Stockholm, Sweden: KTH.

Hacisalihoglu G. & Kochian L.V. (2003) How do some plants tolerate low levels of soil zinc? Mechanisms of zinc efficiency in crop plants. *New Phytologist* 159, 341–350.

Higuchi T. (1982) Gaseous CO_2 transport through the aerencyhma and intercellular space in relation to the uptake of CO_2 by rice roots. *Soil Science and Plant Nutrition* 28, 491–497.

Hoffland E., Wei C. & Wissuwa M. (2006) Organic anion exudation by lowland rice (*Oryza sativa* L.) at zinc and phosphorus deficiency. *Plant and Soil* 283, 155–162.

Impa S.M. & Johnson-Beebout S.E. (2012) Mitigating zinc deficiency and achieving high grain Zn in rice through integration of soil chemistry and plant physiology research. *Plant and Soil* 361, 3–41.

IRRI (2010) *Bringing hope, improving lives. IRRI's Strategic Plan 2007–2015*. International Rice Research Institute, Manila.

Izquierdo M,. Impa S.M., Johnson-Beebout S.E., Weiss D.J. & Kirk G.J.D. (2016) Measuring isotopically-exchangeable Zn in submerged Zn-deficient rice soils. *European Journal of Soil Science* 67, 51-59.

Kirk G.J.D. (2003) Rice root properties for internal aeration and efficient nutrient acquisition in submerged soil. *New Phytologist* 159, 185–194.

Kirk G.J.D. (2004) *The biogeochemistry of submerged soils*. Wiley, Chichester.

Kirk G.J.D. & Bajita J.B. (1995) Root-induced iron oxidation, pH changes and zinc solubilization in the rhizosphere of lowland rice. *New Phytologist* 131, 129–137.

Kirk G.J.D., Versteegen A., Ritz K. & Milodowski A.E. (2015) A simple reactive-transport model of calcite precipitation in soils and other porous media. *Geochimica et Cosmochimica Acta* 153, 108–122

Lane T.W., Saito M.A., George G.N., Pickering I.J., Prince R.C. & Morel F.M.M. (2005) A cadmium enzyme from a marine diatom. *Nature* 435, 42.

Lee J.-S., Wissuwa W., Zamora O.B. & Ismail A.M. (2017a) Biochemical indicators of root damage in rice (*Oryza sativa*) genotypes under zinc deficiency stress. *Journal of Plant Research* doi: 10.1007/s10265-017-0962-0.

Lee J.-S., Sajisi A.G.C, Gregorio G.B., Kretzschmar T., Ismail A.M. & Wissuwa W. (2017b) Genetic dissection for zinc deficiency tolerance in rice using bi‑parental mapping and association analysis. *Theoretical & Applied Genetics* doi: 10.1007/s00122-017-2932-2.

Marković T., Manzoor S., Williams E., Kirk G.J.D., Vilar R. & Weiss D.J. (2017) Experimental determination of equilibrium zinc isotopic fractionation in complexes with the phytosiderophore 2'-deoxymugeneic acid and its structural analogues, and implications for plant uptake mechanisms. *Environmental Science & Technology* 51, 98–107.

McBride M.B. & Blasiak J.J. (1979) Zinc and copper solubility bas a function of pH in an acid soil. *Soil Science Society of America Journal* 43, 866–870.

Mori A., Kirk G.J.D., Lee J.S., Morete M.J., Nanda A.K., Johnson-Beebout S.E. & Wissuwa M. (2016) Rice genotype differences in tolerance of zinc-deficient soils: evidence for the importance of root-induced changes in the rhizosphere. *Frontiers in Plant Science* 6, 1160. doi: 10.3389/fpls.2015.01160.

Nanda A.K. & Wissuwa M. (2016) Rapid Crown Root Development Confers Tolerance to Zinc Deficiency in Rice. *Frontiers in Plant Science* 7, 428. doi: 10.3389/fpls.2016.00428.

Ponnamperuma F.N. (1972) The chemistry of submerged soils. *Advances in Agronomy* 24, 29–96.

Ptashnyk M., Roose T., Jones D.L. & Kirk G.J.D. (2011) Enhanced zinc uptake by rice through phytosiderophore secretion: a modelling study. *Plant, Cell & Environment* 34, 2038–2046.

Quijano-Guerta C., Kirk G.J.D., Bartolome V.I. & Mclaren G.C. (2002) Tolerance of rice germplasm to zinc deficiency. *Field Crops Research* 76, 123–130.

Rose M.T., Rose T.J., Pariasca-Tanaka J., Widodo & Wissuwa M. (2011) Revisiting the role of organic acids in the bicarbonate tolerance of zinc-efficient rice genotypes. *Functional Plant Biology* 38, 493–504.

Rose M.T., Rose T.J., Pariasca-Tanaka J., Yoshihashi T., Neuweger H., Goesmann A., Frei M. & Wissuwa M. (2012) Root metabolic response of rice (*Oryza sativa* L.) genotypes with contrasting tolerance to zinc deficiency and bicarbonate excess. *Planta* 236, 959–973.

Rose T.J., Impa S.M., Rose M.T., Pariasca-Tanaka J., Mori A., Heuer S., Johnson-Beebout S.E. & Wissuwa M. (2013) Enhancing phosphorus and zinc acquisition eefficiency in rice: a critical review of root traits and their potential utility in rice breeding. *Annals of Botany* 112, 331–345.

Saeed M. & Fox R.L. (1977) Relations between suspension pH and Zn solubility in acid and calcareous soils. *Soil Science* 124, 199–203.

Sasaki H., Hirose T., Watanabe Y. & Ohsughi Y. (1998) Carbonic anhydrase activity and CO_2-transfer resistance in Zn-deficient rice leaves. *Plant Physiology* 118, 929–934.

Slamet-Loedin I.H., Johnson-Beebout S.E., Impa S.M. & Tsakirpaloglou N. (2015) Enriching rice with Zn and Fe while minimizing Cd risk. *Frontiers in Plant Science* 6, 121.

Stumm W. &, Morgan J.J. (1996) *Aquatic chemistry. Chemical equilibria and rates in natural waters.* Wiley, New York.

van Breemen N., Quijano C. & Sen L.N. (1980) Zinc deficiency in wetland rice along a toposequence of hydromorphic soils in the Philippines. I. Soil conditions and hydrology. *Plant and Soil* 57, 203–214.

van der Gon H.A.C.D., Kropff M.J., van Breemen N., Wassmann R., Lantin R.S., Aduna E., Corton T.M. & van Laar H.H. (2002) Optimizing grain yields reduces CH_4 emissions from rice paddy fields. *Proceedings of the National Academy of Sciences* 99, 12021–12024.

Widodo, Broadley M.R., Rose T., Frei M., Pariasca-Tanaka J., Yoshihashi T., Thomson M., Hammond J.P., Aprile A., Close T.J., Ismail A.M. & Wissuwa M. (2010) Response to zinc deficiency of two rice lines with contrasting tolerance is determined by root growth maintenance and organic acid exudation rates, and not by zinc-transporter activity. *New Phytologist* 186, 400–414.

Wissuwa M. (2003) How do plants achieve tolerance to phosphorus deficiency? Small causes with big effects. *Plant Physiology* 133, 1947–1958.

Wissuwa M., Ismail A.M. & Yanagihara S. (2006) Effects of zinc deficiency on rice growth and genetic factors contributing to tolerance. *Plant Physiology* 142, 731–741.

Xu S., Zhang X., Guan Q., Takano T. & Liu S. (2007) Expression of a carbonic anhydrase gene is induced by environmental stresses in rice (*Oryza sativa* L.). *Biotechnology Letters* 28, 89–94.

Yoshida S., Forno D.A., Cook J.H. & Gomez K.A. (1976) *Laboratory manual for physiological studies of rice*, 3rd edn. International Rice Research Institute, Manila.

SUPPORTING INFORMATION

Additional Supporting Information may be found in the online version of this article at the publisher's web-site:

Appendix 1: Determination of Zn in soil solutions using isotope dilution mass spectrometry (IDMS)

Appendix 2: Derivation of Zn uptake model

Appendix 3: Model parameter values

Appendix 4: Further soil solution results

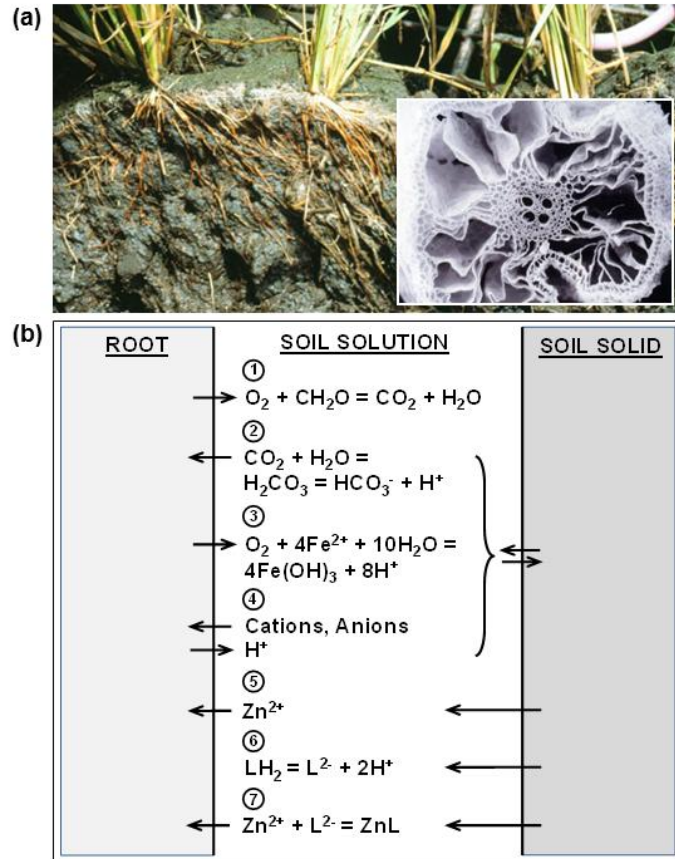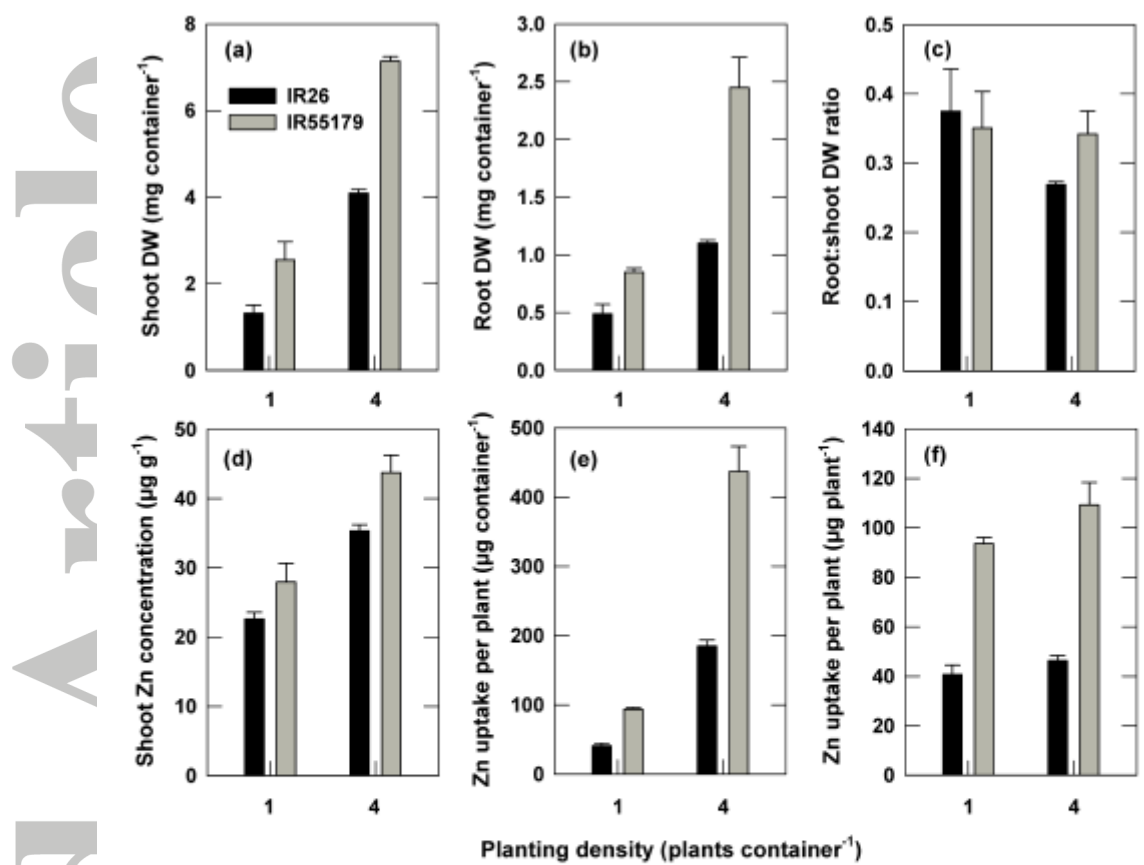**Appendix 5:** Solid solution of $ZnCO_3$ in $MgCO_3$

Figure 1. Root-induced changes in the rhizosphere of rice in water-saturated soil. (a) Rice roots in water-saturated, anoxic soil and (inset) cross-section of a primary root showing aerenchyma. (b) Root effects on the soil:

(1) release of O_2 and organic substrates, represented as CH_2O, from the roots and their consumption in microbial respiration forming CO_2 (note further CO_2 is produced in anaerobic microbial respiration in the soil bulk);

(2) venting of soil CO_2 into the root aerenchyma and associated changes in soil carbonate equilibria;

(3) oxidation of inorganic reductants in the soil, such as ferrous iron (Fe^{2+}), by O_2 from the roots;

(4) excess intake by the root of nutrient cations (particularly ammonium, NH_4^+) over anions and associated release of H^+;

(5) Zn uptake by the root and accompanying desorption and dissolution from the soil solid;

(6) dissolution of organic ligands (L^{2-}) from organic matter in the soil solid, favoured by increases in soil pH;

(7) complexation of Zn^{2+} with organic ligands, increasing the total concentration of Zn in solution and hence increasing Zn uptake.

Note the protons (H^+ ions) consumed or produced in these reactions will be buffered by proton-donating or -accepting groups in the soil solid.

Figure 2. Growth and zinc (Zn) uptake of rice genotypes IR26 and IR55179 in flooded, Zn-deficient soil at two planting densities, 33 d after transplanting seedlings into the soil. (a) Shoot DW per container, (b) root DW per container, (c) root:shoot DW ratio, (d) shoot Zn concentration, (e) total Zn uptake per container and (f) Zn uptake per plant. Data are means ± SE ($n = 3$). The table shows the significance of genotype, density and genotype × density effects for each panel in the figure.

		Nutrient						
	N	K	P	S	Ca	Mg	Fe	Mn
Genotype	***	ns	***	***	***	***	ns	ns
Density	***	***	***	***	***	ns	ns	***
Genotype × density	ns	ns	ns	ns	**	ns	ns	*

ns; *, **, *** = not significant; significant at $P < 0.05$, 0.01 or 0.001
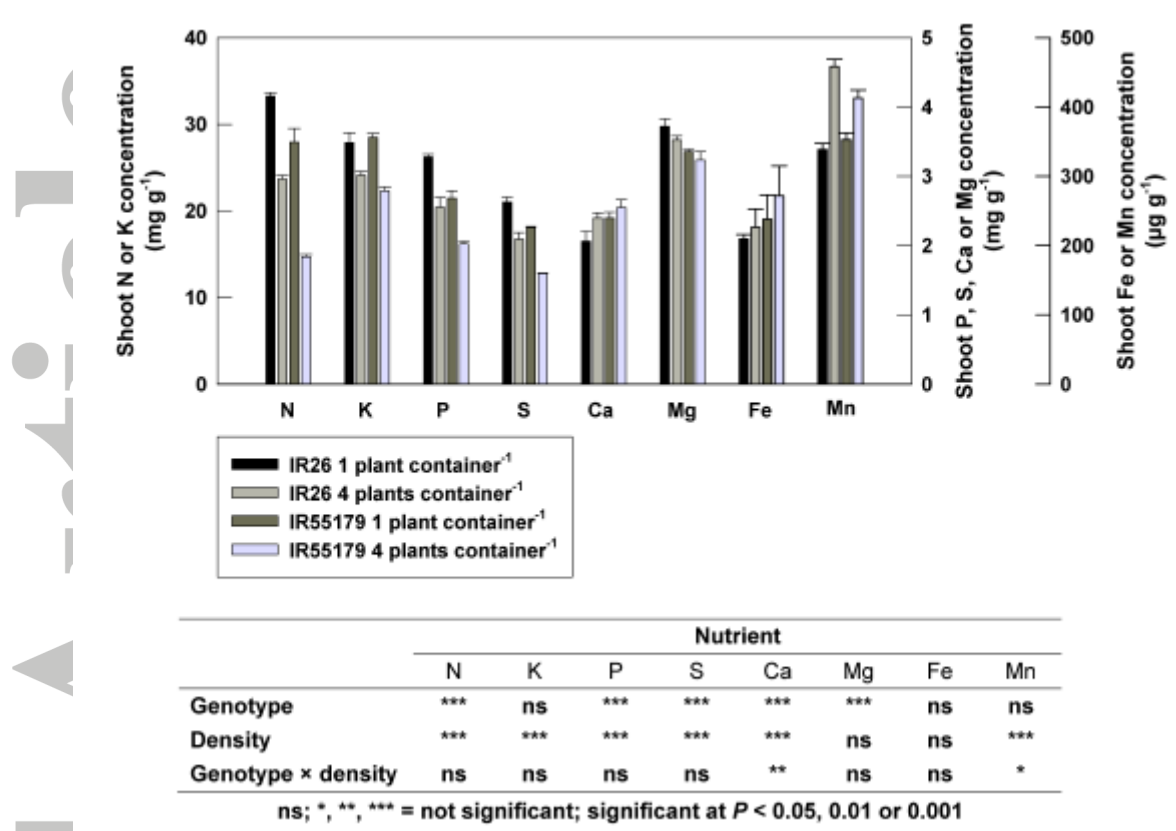
Figure 3. Concentration of macronutrients in plant shoots at 33 d after transplanting in the experiment

shown in Fig. 2. N, nitrogen; K, potassium; P, phosphorus; S, sulphur; Ca, calcium; Mg, magnesium.

Data are means ± SE ($n = 3$). The table shows the significance of genotype, density and genotype ×
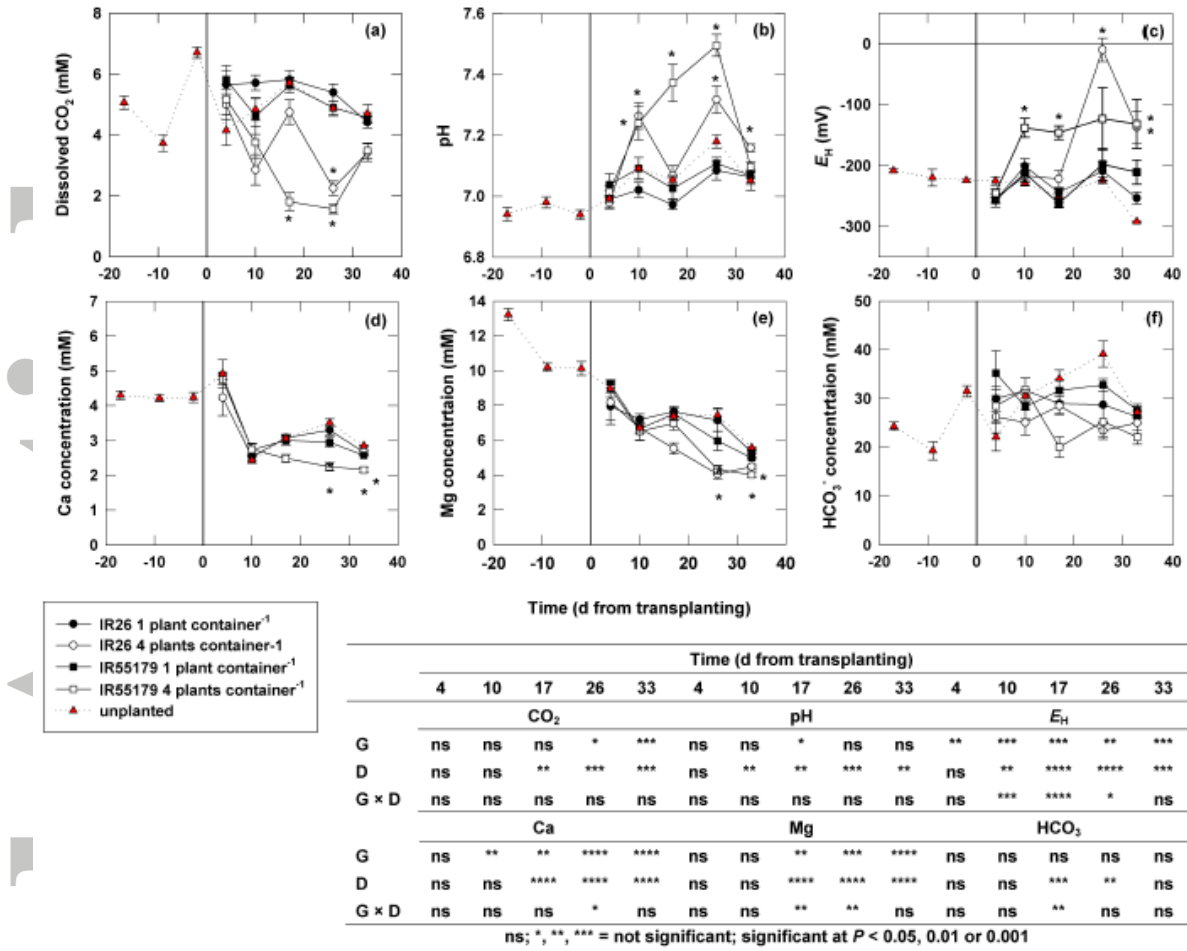
density effects for each nutrient.

	Time (d from transplanting)														
	4	10	17	26	33	4	10	17	26	33	4	10	17	26	33
	CO_2					pH					E_H				
G	ns	ns	ns	*	***	ns	ns	*	ns	ns	**	***	***	**	***
D	ns	ns	**	***	***	ns	**	**	***	**	ns	**	****	****	***
G × D	ns	ns	ns	ns	ns	ns	ns	ns	ns	ns	***	****	*	ns
	Ca					Mg					HCO_3				
G	ns	**	**	****	****	ns	ns	**	***	****	ns	ns	ns	ns	ns
D	ns	ns	****	****	****	ns	ns	****	****	****	ns	ns	***	**	ns
G × D	ns	ns	ns	*	ns	ns	ns	**	**	ns	ns	ns	**	ns	ns

ns; *, **, *** = not significant; significant at $P < 0.05$, 0.01 or 0.001

Figure 4. Time courses of the composition the soil solution for the experiment shown in Fig. 2. (a) Dissolved CO_2, (b) pH, (c) E_H, (d) calcium (Ca), magnesium (Mg) and (f) bicarbonate (HCO_3^-). Data are means of three solution samplers and three replicate containers ± SE ($n = 9$). The table shows the significance of genotype (G), density (D) and genotype × density effects.
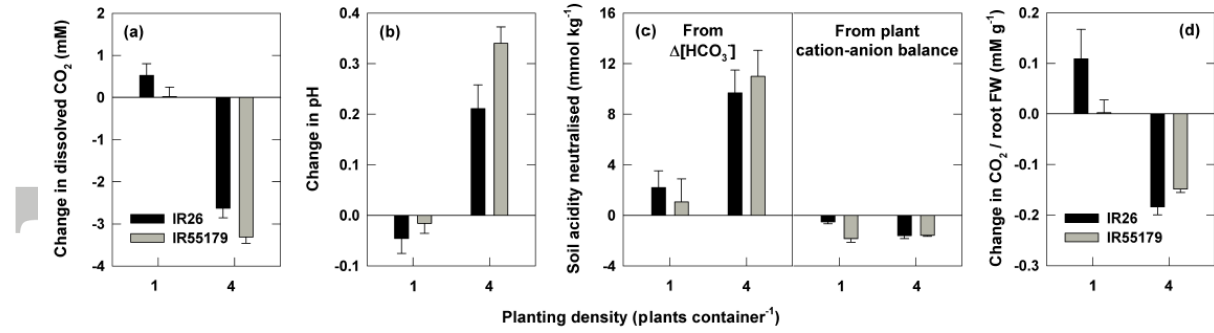
Figure 5. Changes from the unplanted soils in: (a) dissolved CO_2, (b) pH, (c) soil acidity and (d) dissolved CO_2 relative to root FW. The changes in soil acidity were calculated from the changes in bicarbonate ($\Delta[HCO_3^-]$) and the plant cation-anion balance as described in the text. Data are means ± SE ($n = 9$) at 26 d after transplanting

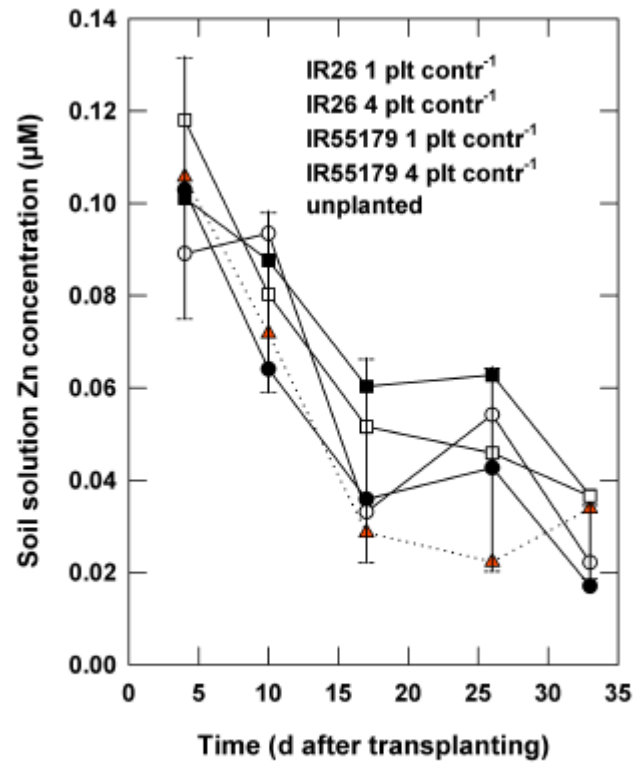**Figure 6.** Time courses of Zn concentration in the soil solution. Data are means ± SE (n = 3). Error bars are $LSD_{0.05}$ for pooled data at each time.
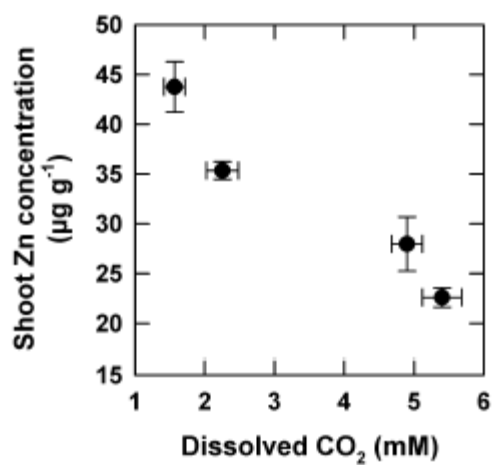
Figure 7. Relation between total plant Zn uptake and the dissolved CO_2 concentration in the soil solution at 26 DAT. Data are means $\pm$ SE ($n = 9$ for $[CO_2]$ and 3 for shoot Zn).
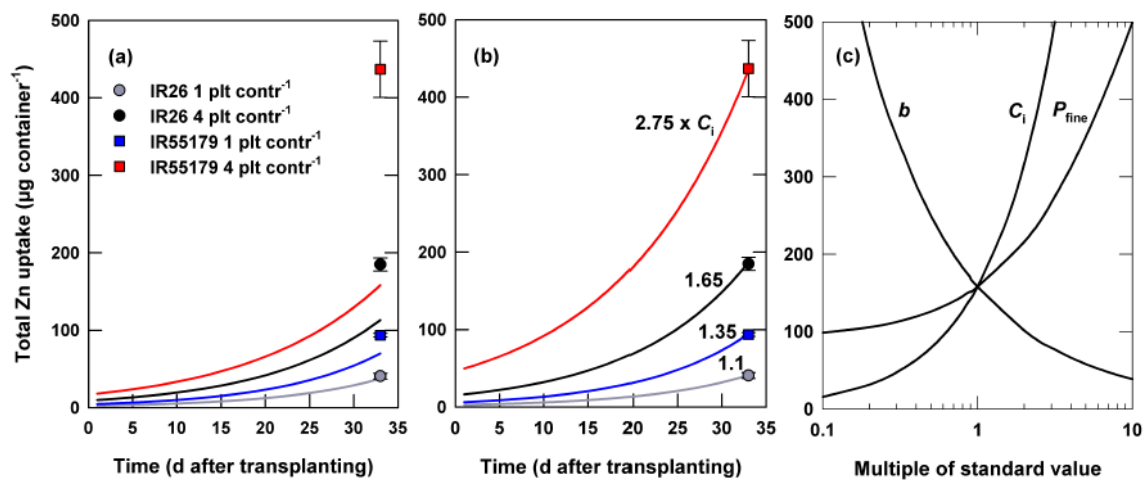
Figure 8. Results of modelling to test the null hypothesis that the effects of planting density and genotype on uptake do not depend on plant-induced solubilisation of soil Zn. Points are measured data (means ± SE); lines are model results (a) for the standard parameter values measured on the experimental soil and plants (Appendix 3), and (b) for the standard parameter values with the plant-available Zn concentration (C_i) multiplied by the indicated factors. (c) The sensitivity of the predicted uptake by the tolerant genotype IR55179 at 4 plants container^{-1} to the soil Zn buffer power (b), the concentration of readily plant-available Zn in the soil (C_i) and the proportion of root FW as fine roots (P_{fine}). In (c), the indicated parameters are varied in turn with all other parameters held at their standard values; note the x-axis is logarithmic.